A computational study of necking and drawing of plastic-rubber laminates

Rahul G. Ramachandran, Spandan Maiti and Sachin S. Velankar, University of Pittsburgh, Pittsburgh, PA

Abstract

Semi-crystalline plastics undergo necking followed by stable drawing under tensile forces. In contrast, a rubber extends many times its original length uniformly under tension. Previously we have shown experimentally that the behavior of rubber-plastic composites in tension is intermediate between that of the rubber. Here we conduct finite element simulations of plastic-rubber-plastic trilayers laminates under tension. Using relatively simple constitutive equations for the rubber and the plastic, we examine how the composite mechanics changes as the ratio of rubber to plastic thickness is varied. We show that at small rubber thickness, the composites show necking, whereas beyond a certain rubber thickness, necking is completely eliminated.

Introduction

When subjected to tension, semi-crystalline polymers under suitable strain rate and temperature conditions undergo necking followed by stable neck propagation, a phenomenon sometimes called cold drawing[1]. Cold drawing causes increase in the modulus of the material by realigning the crystalline phase along the direction of tensile loading. Making this a process that find wide application in polymer industry.

In contrast, elastomers when subjected to tension extends elastically, thinning uniformly. An interesting question therefore is the mechanical behavior of rubber-plastic laminate composites comprising layers that are capable of necking and drawing and that stretch homogeneously.

Previously we showed experimentally that the necking and drawing behavior can be modified by the addition of a rubber layer[2]. Here we examine the same situation using a finite element based computational approach. Specifically, we conduct 3D simulations of rectangular bars of plastic-rubber-plastic trilayer composites under tensile loading to examine their necking and drawing behavior.

Background

A semi-crystalline material is typically composed of a spherulitic crystalline phase and an amorphous phase. Cold drawing involves breaking down of the spherulite crystalline structure and re-alignment of the crystalline lamellae along the direction of tensile loading [3]. In a uniaxial tensile test, the nominal stress corresponding to the initiation of the breakdown process is regarded as the *yield stress* of the material. Once the breakdown is initiated, only a relatively small increment of true stress is required to completely re-orient the crystalline material along the loading direction. In tensile loading, this stress increment during re-alignment does not compensate for the increase in the stress due to cross-sectional area reduction that happens due to Poisson contraction. Hence, such materials, when subjected to tension, a local instability called necking could be triggered.

A neck can initiate at any location where the stress is higher than yield stress. Typically, such initiation occurs at some "defect" location where the local stress is high due to inhomogeneity in material properties, or inhomogeneity in the geometry. Since formation of a neck locally reduces the cross section of the material, this translates into a larger local stress in the neck. This in turn raises the local strain. which further reduces the local cross sectional area due to Poisson contraction. This phenomenon of runaway necking instability, also called strain localization, generally leads to failure. However, cold drawing materials do not neck to failure. Once the realignment in the neck finishes, the modulus, i.e., the stress increment required for unit strain increment increases multifold. Such strain hardening acts as a stabilizing mechanism. The nominal stress corresponding to the completion of crystalline re-alignment in the neck is called the draw stress, and the corresponding local stretch is called the natural draw ratio of the material[4]. Once the nominal stress has reduced to the draw stress, further deformation is accommodated by pulling more material into the necked state at a constant nominal stress, a process called neck propagation. Once the neck has propagated throughout the material, the specimen can start stretching homogeneously.

In the above discussion, the strain hardening that stabilizes the neck is an internal phenomenon for the material. However, this need not be the case. One may instead bond the semi-crystalline plastic to a separate strain hardening layer that can serve the same function of stabilizing the neck. A hyper elastic material that is soft at small values of strain and shows strong strain hardening at large values of strain would be an ideal candidate for this function.

We recently examined the tensile behavior of bilayer composites comprising a polymeric plastic layer (linear low density polyethylene, LLDPE) bonded to an elastomer (styrene-ethylene/propylene-styrene, SEPS). behavior of films of the rubber and the plastic, as well as bilayer composite films with various layer thickness were examined. The spatial deformation of the specimens was quantified by video analysis of the tensile tests. The chief experimental observations were as follows, (i) with an increase in rubber thickness, the natural draw ratio of the composites reduced as compared to the free-standing plastic. (ii) The force needed for stable drawing increased with increase in rubber thickness (not surprising since the overall composite thickness increased), (iii) but the average draw stress decreased. (iv) At sufficiently large rubber thickness the deformation became nearly homogeneous, i.e. necking behavior was nearly eliminated.

In this work, we use Finite Element modeling of a laminate system composed of a cold drawing material and elastomer to examine this same situation in greater detail. Unlike the experimental study, simulations allow accessing the local stresses in the sample, as well as the stress in individual layers. These provide insights into the large deformation behavior of rubber-plastic composites.

Methods

The deformation and stress response of rubber and plastic material as free-stranding layers as well as their laminates was studied using a custom developed non-linear finite element program. The specimen was a long rectangular film of size $80 \times 6 \,mm$. Due to symmetry, only one eighth of plastic-rubber-plastic trilayer laminate was modelled, and roller boundary conditions were enforced on faces in the x, y and z direction, shown in Figure 1. Thickness of each layer of the plastic film was kept at 50 microns and the rubber thickness was varied from 10 to 800 microns. The geometry was meshed using 8 noded brick elements. A blunt notch of radius 0.1 mm was introduced in the symmetry plane along the length of the specimen (x-direction) to consistently introduce necking in the middle. Radial elements were employed near the notch tip to capture the stress concentration. Each layer has 8804 elements and at least 2 layers of mesh was paved along the thickness. The model was displaced to a nominal stretch of 7 in 12000 steps.

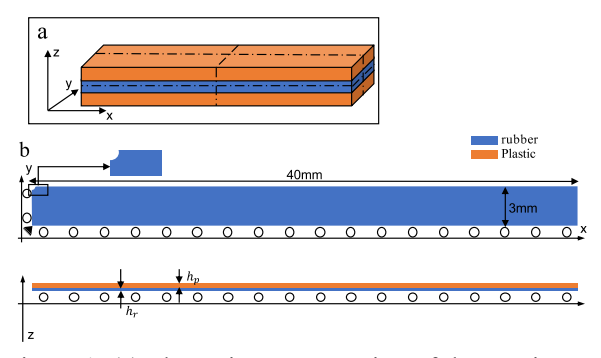


Figure 1. (a)schematic representation of the specimen. (b) finite element model shown in top view and cross-sectional view. h_r and h_p are the thickness of rubber and plastic layer respectively. The blunt notch is shown in the inset

The mechanical response of a cold drawing plastic layer is assumed to be composed of an elasto-plastic part and a nonlinear elastic part. This approach was inspired from the structure of semi-crystalline polymers which are composed of crystalline parts which deform in an elasto-plastic fashion and amorphous phase which deform in a hyper elastic fashion.

The elastic constitutive response of the crystalline phase of the plastic material was chosen to be governed by the incompressible neo Hookean strain energy function:

$$\mathbf{W}_{crystalline}^{p} = C_1(\mathbf{I}_1 - 3) \tag{1}$$

where I_1 is the first invariant of the Green-Cauchy deformation tensor. Further the yield surface of the crystalline phase was defined by

$$\sqrt{\frac{3}{2}\mathbf{M}_d^e:\mathbf{M}_d^e} - (\sigma_y + H\overline{\epsilon}_p)$$
 (2)

where \mathbf{M}_d^e is the deviatoric part of Mandel stress tensor. σ_y is the yield stress in the current configuration, H is the hardening modulus and $\overline{\in}_p$ is the plastic strain.

The amorphous phase was defined by an incompressible elastic strain energy function of the form,

$$\mathbf{W}_{amorphous}^{p} = C_2(\mathbf{I}_1 - 3)^2 \tag{3}$$

The material parameters were assigned as $C_1 = 50MPa$, $\sigma_y = 18MPa$, H = 15MPa, $C_2 = 0.006MPa$ which is in rough agreement with the materials examined experimentally. The nominal stress strain response of the plastic is given in Figure 2. The draw stress of 12 MPa and natural draw ratio of around 6 are both rough agreement with the of LLDPE used in our previous research[2].

The strain energy function of rubber was taken as

$$\mathbf{W}^r = C_3(\mathbf{I}_2 - 3) + C_4(\mathbf{I}_1 - 3)^2$$
 (4)

where I_1 and I_2 are the first and second invariant of the Green-Cauchy deformation tensor. $C_3 = 2 \, MPa$ and $C_4 = 0.014 \, MPa$ were the values of the parameters, which is in rough agreement with those needed to model the SEPS rubber used experimentally[2]. The nominal stress stretch response of the rubber for the given parameters is also shown in Figure 2.

Results

The simulated nominal stress-stretch behavior of the plastic shown in Figure 2 follows the general description of a cold drawing material discussed in the introduction. The curve has following features. An initial elastic part where the stress reaches a maximum, followed by a sharp reduction in stress with applied stretch. Further deformation then proceeds at a constant stress. Later we will show (Figure 3) that the peak in stress corresponds to neck initiation and the plateau corresponds to stable drawing. The plateau continues till the specimen is completely converted to necked state. The small dip in stress seen at stretch of around 5.5 is due to the geometric softening (i.e. decrease in cross sectional area at the edge where the force is calculated) when the neck reaches the edge of the specimen. Such a dip would not be seen experimentally when dog-bone shaped specimens are used. In contrast to the complex stress-strain behavior of the plastic, the rubber in Figure 2 shows a monotonic increase in nominal stress with applied stretch.

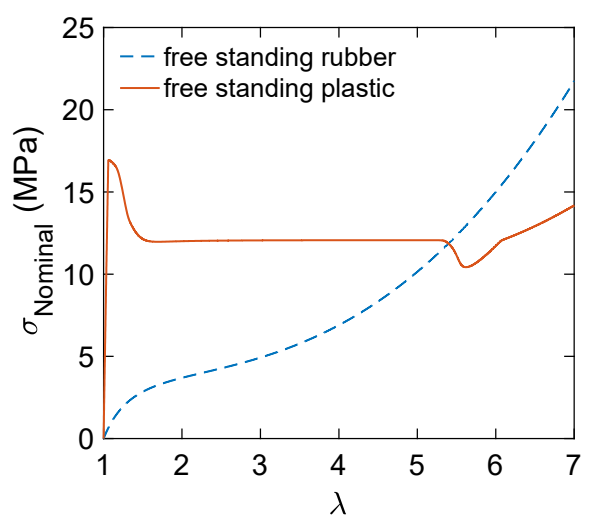


Figure 2. The simulated nominal stress-stretch response of rubber and plastic.

Figure 3 shows snapshots of the geometry of the plastic during deformation at applied stretches of 1.1, 1.3, 1.6, 2, 3, 4, 5, 6. The color maps are the stretch at the top

free surface. Note that only one eighth of the geometry is shown since all other features are symmetric about the x,y and z direction.

At an applied stretch of 1.1 (Figure 3b), the stretch contour has an almost uniform color everywhere on the specimen surface, except in the region in close vicinity of the rounded notch (not discernable in the figure). This signifies homogeneous deformation throughout the specimen. With a further increase of applied stretch to $\lambda_{app} = 1.3$, the deformed geometry starts showing localized deformation at the left end. When applied stretch is increased to 1.6 (Figure 3d), three distinct regions can be identified from the stretch color map and the deformed shape. The first region is to the left end, where the stretch has a large value compared to rest of the geometry, indicated by the warm red color in stretch contour. The second is the region towards the right end where the material remains in nearly the same state prior to necking and is called the unnecked region. The third is the transition region between the aforementioned zones, where the value of the stretch smoothly transitions from the value in necked region to the value in the unnecked region. With further increase in the applied strain, these three regions persist with no change in the stretch of any of the necked or unnecked region or the shape of transition zone. The sole difference between Figures 3e-h is the increase in the necked region at the expense of the unnecked length. Thus, this regime of stretching corresponds to stable drawing. Finally, at $\lambda = 6$ the entire specimen is uniformly stretched, because at this applied stretch the entire specimen has transformed from unnecked state to necked state. Beyond this, the sample stretches homogeneously.

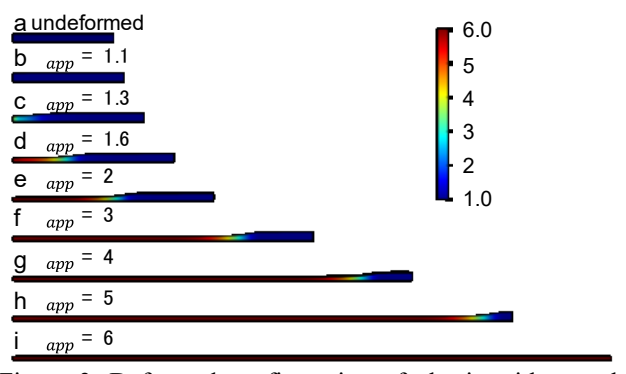


Figure 3. Deformed configuration of plastic with stretch contour at various instance of applied stretch.

The deformed configuration and the stretch contour on the rubber surface at discrete instances of applies stretch is shown in Figure 4. Uniform stretch contour at each applied stretch suggests that the deformation is homogeneous in the elastomeric material. Further the magnitude of stretch as indicated by the color of the stretch contour is equal to the applied stretch.

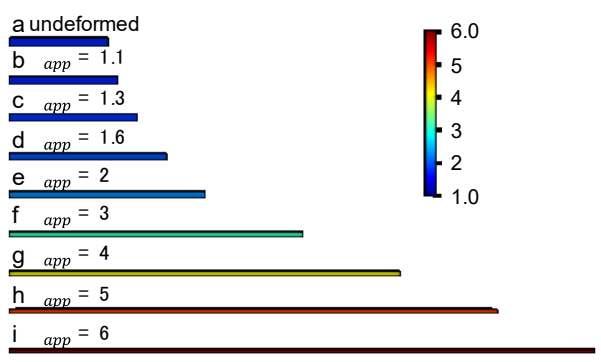


Figure 4. Deformed configuration of rubber with stretch contour at various instance of applied stretch.

The deformation profile and the stretch in the plastic-rubber-plastic trilayer with rubber:plastic thickness ratio of 1 is shown in Figure 5. Qualitatively, the shape evolution of the sample resembles that of the plastic: an early phase of stretching during which the sample stretches homogeneously, followed by neck initiation, followed by a stable drawing regime during which the three regions (necked, unnecked, and transition) can be identified. Once the entire sample necks, the deformation becomes homogeneous. Yet, there are clear quantitative differences: (1) the neck initiates later during the deformation ($\lambda = 1.6$ in Fig. 5 vs $\lambda = 1.3$ in Fig. 3); (2) the stretch associated with stable drawing reduces (3.8 in Fig. 5 vs 6 in Fig. 3), (3) the sample reverts to homogeneous deformation at a smaller stretch (3.8 in Fig. 5 vs 6.0 in in Fig. 3, and finally it is also observed that the width of the transition zone is larger in the composite as compared to the plastic alone.

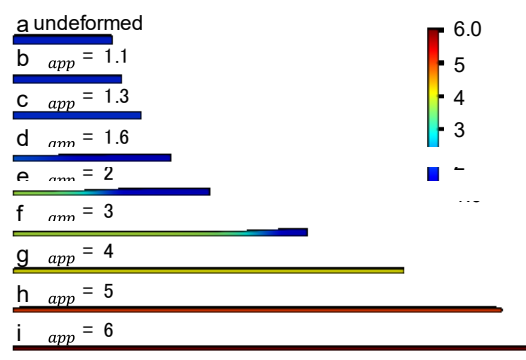


Figure 5. Deformed configuration and the stretch profile at various instance of applied stretch for plastic-rubber-plastic tri-layer of rubber/plastic thickness ratio of 1.

Simulations were conducted at a variety of other rubber:plastic ratios and qualitatively their deformation behavior was similar to that shown in Figure 3 and 5 when the rubber-plastic thickness ratio $h_r/h_p \le 2$. In contrast, deformation became homogeneous and similar to that of a rubber for $h_r/h_p \ge 3$.

Discussion

We will now quantify the degree of non-homogeneity of deformation in the various samples. Perhaps the easiest way of judging inhomogeneity is to take the ratio $\lambda_{max}/\lambda_{min}$ where λ_{max} and λ_{min} are maximum and minimum stretch measured along the centerline of the simulated specimen. Figure 6 plots the $\lambda_{max}/\lambda_{min}$ vs the applied stretch for all the samples. The rubber, and composites with values of $h_r/h_p \geq 3$ have this ratio equal to 1 throughout the deformation process indicating homogeneous deformation. Samples with a $h_r/h_p \leq 2$ show $\lambda_{max}/\lambda_{min}$ increase sharply (indicating the onset of necking), a plateau (stable drawing), and then a decrease (when the neck has propagated throughout the sample).

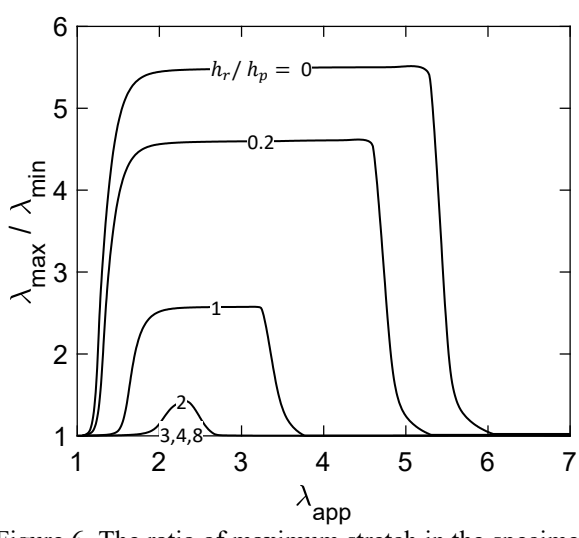


Figure 6. The ratio of maximum stretch in the specimen to the minimum stretch in the specimen is plotted against applied stretch

In our previous experimental research [2], we defined the inhomogeneity index as,

Inhomogeneity Index = highest value of
$$\frac{\lambda_{max}}{\lambda_{min}}$$

during the entire deformation. This index offers a single number that can compare the non-homogeneity of deformation of all samples. We will adopt the same index for the simulation results. The inhomogeneity index corresponding to Figure 6 is shown in Figure 7. It shows that as the rubber-plastic thickness ratio is increased the deformation changes from highly inhomogeneous to homogeneous deformation. Furthermore, the transition from inhomogeneous to homogenous deformation happens for rubber-plastic thickness ration between 2 and 3.

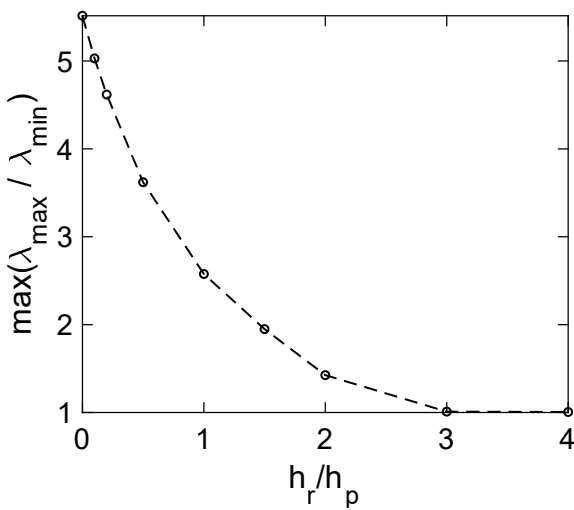


Figure 7. The maximum of the ratio of maximum stretch in the material to the minimum stretch in the material (*Inhomogeneity Index*) is plotted against the rubber plastic thickness ratio

It is also interesting to examine how the rubberplastic thickness ratio affects the stretch in the necked and the stretch in the un-necked region during stable drawing (Figure 8). As the rubber thickness is increased, the steady state stress in the neck decreases rapidly. Also, the stretch in the unneck region increases suggesting delay in the onset of necking with increasing rubber-plastic thickness ratio.

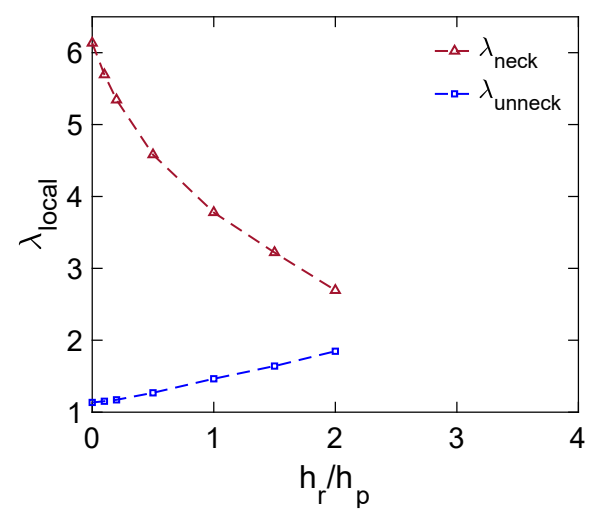


Figure 8. The steady state stretch in the neck and un-neck zone plotted against the rubber plastic thickness ratio. The laminate does not show necking or drawing for rubber plastic thickness ratio greater than 2, hence no data is reported in this range.

Summary and Conclusions

When the plastic film in free-standing form was stretched, the material deformed uniformly at small applied

stretch values and then localized near the notched end as shown by the stretch contours in Figure 3 and the ratio of maximum to minimum stretch in the material shown in Figure 6. The stretch in the necked region then saturated and further deformation progressed by the transformation of un-necked material to necked along the length of the specimen by the movement of the transition zone. The stretch in the neck (often called the natural draw ratio) during the steady state drawing was around 6.0 whereas the stretch in the un-neck region was just around 1.1.

It was seen that the addition of rubber modifies the local stretch response of the plastic layer. The stretch distribution along the length of the specimen in Figure 3-5 and inhomogeneity index shown in Figure 7 suggests that behavior of the laminates remained qualitatively similar to that of a free-standing plastic for composite of $h_r/h_p \le 2$. However, the following differences where apparent. The addition of rubber on plastic delayed the onset of localized deformation; reduced the saturation stretch in the neck during steady state and consequently caused the material to revert to homogeneous deformation at a lower value of applied stretch. This is reflected in the Figure 6 as lowering of the ratio of maximum to minimum stretch in the material during steady state drawing. Also, the stretch in the neck reduced to around 3.8 with a rubber addition of equal thickness to the plastic (Figure 8).

Figure 7 suggest that the measure of inhomogeneity in the material drops sharply with rubber thickness. Further, the composite assumes completely homogeneous deformation for rubber/plastic ratio between 2 and 3, a critical limit for achieving homogeneous deformation for the chosen material models. In summary, this simulation method can be pursued further (to be published) to examine in detail the mechanics layered composites with a further focus on how material properties affect composite behavior.

References

- Wallace H. Carothers, J.W.H., Studies of Polymerization and ring formation. XV. Artificial fibres from synthetic linear condensation superpolymers. Communication No. 78 from the experimental station of E I Du Pont De Nemours & Co, 1932.
- Ramachandran, R.G., et al., Necking and drawing of rubber-plastic bilayer laminates. Soft Matter, 2018. 14(24): p. 4977-4986.
- 3. Argon, A.S., *The Physics of Deformation and Fracture of Polymers*. 2013, New York: Cambridge University Press.
- Ward, I.M., Mechanical Properties of Solid Polymers, in Mechanical Behavior of Solid Polymers. 1971, J. W Arrowsmith Ltd: Bristol. p. 321 - 394.